ANTIBACTERIAL AND PHOTOCATALYTIC ACTIVITIES OF ZnO NANOPARTICLES: SYNTHESIS VIA COMBUSTION METHOD

Danith kumar[1], L.S. Reddy Yadav[1], K. Lingaraju[2], H. Raja Naika[2], K. Manjunath[3], D. Suresh[4], H. Nagabhushana[5] , S.C. Sharma[6] and G. Nagaraju[*1]

[1]*Dept. of Chemistry, BMS Institute of Technology, Avalahalli, Bangalore*

[2]*Dept. of Studies and Research in Environnemental Science, Tumkur University, Tumkur*

[3]*Centre for Nano and Material Sciences, Jain University, Jakkasandra, Kanakapura (T)*

[4]*Dept. of Studies and Research in Chemistry, Tumkur University, Tumkur*

[5]*CNR Rao Center for Advanced Materials, Tumkur University, Tumkur*

[6]*Chattisgarh Swami Vivekananda technological University, Bhilai*

*Corresponding author: E-mail: nagarajugn@rediffmail.com

Abstract - In the present work, Zinc Oxide nanoparticles (ZnO Nps) have been prepared by a simple solution combustion method using Zinc nitrate as a precursor and grape juice as a fuel. The structure and morphology of the synthesized ZnO Nps were analyzed using X-ray diffraction (XRD), Fourier Transform Infrared spectroscopy (FTIR), UV-Vis spectroscopy, Photoluminescence (PL) spectroscopy, Scanning Electron Microscopy (SEM). XRD pattern indicates that the prepared product belongs to hexagonal wurtzite structure. The FT-IR spectrum of ZnO Nps shows significant spectroscopic band at 416 cm^{-1} associated with the characteristic vibrational mode of Zn–O bonding. The UV-Vis spectrum shows a maximum absorbance at 371 nm. The band at 502 nm in the in the yellow region is due to the intrinsic defects of oxygen vacancies. SEM images showed that the prepared particles were agglomerated to form loofa like structure. ZnO NPs shows good photocatalytic activity for the degradation of methylene blue (MB) dye, as well as significant antibacterial activities against four pathogenic bacterial strains.

Keywords: Nanoparticle, Combustion, Photodegradation, Microbial activity

I. INTRODUCTION

In current days nanoscale materials have been widely studied due to their interesting physical and chemical assets, associated to their bulk materials [1]. Among nanomaterials of transition metal oxides, ZnO is considered as a significant material for multiple applications including catalytic, optical, magnetic, electrical, electrochemical and biological assets. These properties makes ZnO as a multifunctional material that finds applications in solar cell, biosensors, field effect transistors, light emitting diodes, diluted and ferromagnetic materials for spinctronics, photocatalysis and anti-bacterial activity[2]. ZnO is a direct band gap (3.37eV) semiconducting materials with a large exciton binding energy of 60meV [3-6]. It is one of the strongest material in the II-IV compound family. As a result ZnO do not undergo dislocation degradation during synthesization [7]. ZnO has various kinds of morphologies such as nanoneedles, nanobelts, nanoflowers, nanorods, nanobows, nanonails, nanoparticles and nanowires [8]. Different methods have been followed to synthesize ZnO nanomaterials such as chemical precipitation [9-10], sol-gel [11], solvothermal, [12], hydrothermal [13-14], electrical and photo-chemical reduction techniques [15-16], co-precipitation [17-18], polymerization method [19], laser ablation [20], sonochemical [21-22], etc. Most of these methods entail expensive substrates, deadly process, cultured equipment's, difficult experimental conditions, etc. Solution combustion synthesis is a version of simple and easier method to prepare most of the metal oxides. It presented with time and energy saving prospect. In this direction, combustion method is an ideal method as it ensures uniform distribution and atomic

level mixing of reactants with an ignitable fuel to produce phase pure final product in the form of ultra-fine powder with reducible particle size. Again the fuel plays very important role as it is responsible for the liberation of energy to produce soft mass in combustion method. Solution combustion is an exothermic redox reaction between metal nitrates (oxidizing agent) with an appropriate fuel (reducing agent) and had been successfully used to synthesize nanocrystalline metal oxides[23-26] Many researchers have used commercially available carbohydrates and amines as a combustible fuel for the preparation of metal oxides/alloys [27-28]. Sumana et al. [28] have synthesized ZnO nano powder using sugar as a fuel. Rausli et al. [29] have used urea as a fuel to prepare nanocrystalline ZnO. Relatively different from conventional methodologies peoples have used naturally occurring compounds as a fuel for the preparation of nanocrystalline materials for eg. Kalyani et al. [30] synthesized $LiCoO_2$, $LiMn_2O_4$ and $LiNiVO_4$ using rice starch as a fuel.

In this paper, we have reported the synthesis of ZnO Nps using grape juice as a fuel for the first time. The obtained product was characterized and tested for photo catalytic and antibacterial activity.

Grape juice (Vitis vinifera) belongs to vitaceae family that could play an significant role as combustible fuel. It comprises high level of acetic-acid, alpha-carotene, alpha-linolenic-acid, alpha-tocopherol, anthocyanins, arginine, ascorbic-acid, benzoic-acid, beta-carotene, beta-sitosterol, caffeic-acid, calcium, chlorogenic-acid, chromium, cinnamic-acidcitric-acid, coumarin, ellagic-acid, epicatechin, ferulic-acid, fiber gaba, gallic-acid, geraniol linoleic-acid, luteinlycopene, magnesium, niacin, pectin, potassium procyanidins, quercetin, resveratrol, selenium, tryptophan, and zinc. Taking this in to an account a novel attempt to exploit naturally occurring grapes as fuel has been proposed to synthesize ZnO nano powder. This procedure involves a self-sustained reaction in homogeneous solution of Zinc nitrate as an oxidizer and grape juice as fuel.

II. EXPERIMENTAL

A. Synthesis

The solid grape juice was prepared by grinding grapes and filtered to remove the impurities. 2.97g of zinc nitrate [$Zn(NO_3)_2.6H_2O$] was dissolved in 5ml of solid grape juice and 10 ml of water and stirred for about 10 min to get homogeneous solution. This solution is kept in a pre-heated furnace maintained at about 400 ^oC. Smoldering type of the reaction takes place with the liberation of gases and within 3-4 min, nanocrystalline ZnO is obtained. The obtained product was calcined at the same temperature (400 ^oC for 3hours) and to remove the impurities. Finally the milky white ZnO nanomaterial is obtained. The synthesized ZnO was characterized by XRD, FTIR, UV-Vis, PL, SEM, TEM and used for photo degradation and antibacterial activity.

B. Characterization

The powder X-ray Diffraction data was analyzed by SHIMADZU 700 X-ray diffractometer with graphite monochromatized Cu-Kα (1.5418 Å) radiation. The Fourier transform infrared spectrum of the sample is collected using Bruker Alpha-P spectrometer. The absorption spectrum of the sample was measured on a SHIMADUZU UV- 1800 UV-Vis spectrometer. Photoluminescence studies were carried out by HORIBA luminescence spectrometer equipped with Xenon lamp with excitation wavelength of 350 nm at room temperature. The morphology of the samples was examined using HITACHI 7000 Table top Scanning electron microscope and JEOL JEM 1200 Ex operating at 100 kV Transmission electron microscopy.

C. Photocatalytic degradation of organic dyes

Photo catalytic experiments were carried out in a 150X75 mm batch reactor. An aqueous suspension was prepared by dispersing 100 mg of ZnO nanoparticles in 100 ml of 10 ppm Methylene blue dye solution. During the photo Catalytic experiments the slurry composed of dye solution and catalyst was placed in the reactor and stirred magnetically for agitation with simultaneous exposure to Sun light or UV light. Known volume (10 ml) of the exposed solution is withdrawn at specific interval of time (30 min). ZnO nanoparticles were removed from the solution by centrifugation to assess the extent of degradation. . The % of degradation can be determined using the following formula shown in the Equation 1.

$$\% \text{ of degradation} = \frac{C_i - C_f}{C_i} \times 100$$

C_i and C_f are the initial and final concentrations of dye. The experiment was carried out by varying experimental parameters like concentration of dye, catalytic load, irradiation time, pH and nature of light, etc.

D. Evaluation of antibacterial activity

Anti-bacterial activity was carried out by agar well diffusion method[31] and broth micro dilution method [24,25] against a gram –ve bacteria *klebsiella aerogenes* NICM 2098, *Escherichia coli* NCIM-5051, *pseudomonas aeruginosa* NICM-2242 and gram +ve bacteria *staphylococcus aureus* MCIM-5052. Nutrient were prepared under sterile condition

and spread plate method using sterile L- shaped glass rod with 100µl of 24 hrs old broth culture of respective bacterial strains. Using the germ-free cork barber, the well (6mm) was made into the each petri-plate. Various concentrations of nano materials (ZnO) (500 and 1000µg/well), were used to assess the dose dependent activity of the compounds. The compounds were prepared in sterile water added into the wells by using sterile micropipettes. Concurrently the standard antibiotic (as positive control) was tested against the bacteria. Ciprofloxacin (Hi media, India) was used as positive control. Then the plates were incubated at 37 ^{o}C for 36 hrs. Later the incubated period, the zone of inhibition of each well was measured and the values were noted. Triplicates were maintained in each compound and the average values were calculated for the eventual anti-bacterial activity. The broth micro-dilution method was done for antibacterial activity. The nanomaterial (ZnO) was watered down with germ-free water to get two different concentrations of the sample solutions (i.e. 200 and 400 µg/mL). Then these sample solutions were added into germ-free tubes containing nutrient broth and 0.1 mL of bacterial suspension (~108 CFU/mL) was added into each tube. In addition, positive control tubes containing the same amount of bacterial cell and nutrient broth and negative control tubes containing only nutrient broth were organized, respectively. All the tubes were incubated in a reciprocal shaker (Tarsons, Mumbai) with a shaking speed of about 200 rpm/min at 37 °C for 24 hrs. The MIC was determined as the minimum concentration at which there is no visible change in the turbidity of the medium. To evaluate the bactericidal efficacy of the samples, 0.025 mL each of the bacterial solution with 200 and 400 µg/mL samples were taken and plated in germ-free nutrient agar plates. Then the plates were incubated at 37 °C for another 24 hrs, and the number of bacterial colonies was counted. The bactericidal rate (K) could be calculated according to the following equation.

$$K = \frac{A - B}{B} X \ 100$$

Where A and B are the number of bacterial colonies corresponding to the positive control group and the sample group, respectively.

III. RESULTS AND DISCUSSIONS

The figure1 shows the XRD pattern of ZnO nanoparticles prepared via combustion method using grape juice as fuel. All the diffraction peaks are matches well with the hexagonal wurtzite crystal structure of ZnO with cell constants a = b= 3.253 Å and c = 5.213 Å (JCPDS no.89-1397). There are no other peaks matching to any secondary or impurity phase were observed which indicates the phase concentration of the sample. The average crystallite size was Assessed by the Debye-Sherrer's formula was found to be 53nm.

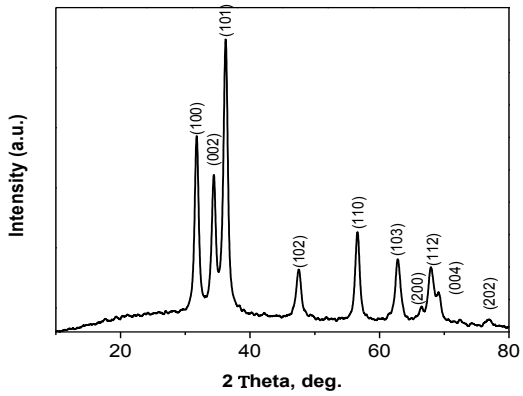

Fig.1 XRD pattern of ZnO nanoparticles

$$D = \frac{0.9 \lambda}{\beta \cos \theta}$$

Where D is the crystal size and λ is the wavelength of X-ray radiation (1.5418 Å), β is the full width half maximum of diffraction peak and θ is the scattering angle.

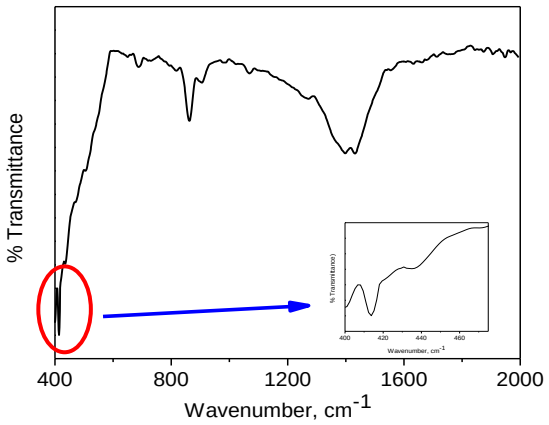

Fig.2 FTIR spectrum of ZnO nanoparticles

The purity and molecular structure of product were analyzed by the FTIR spectroscopy. Fig.2 shows the FTIR spectrum of the ZnO nanocrystalline powder which was acquired in the range of 400- 2000cm^{-1}. The two peaks at 1434 and

1395 cm^{-1} are attributed to O–H stretching vibration and the peak at 861 cm^{-1} are attributed H–O–H bending vibration, which are assigned to small amount of H_2O existing in the nanocrystalline ZnO. The peak at 416 cm^{-1} is ascribed to Zn–O stretching vibration. No other impurity peaks related to other groups are observed which shows the purity of the sample.

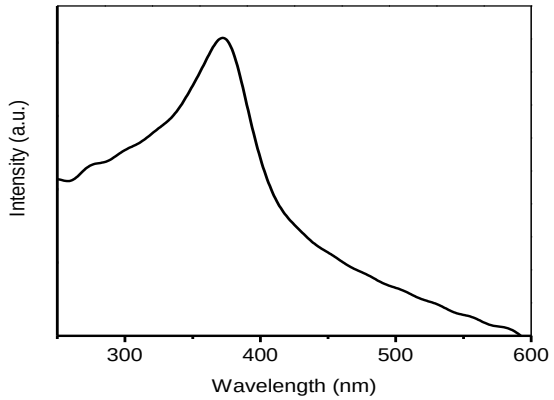

Fig.3 UV-Visible spectrum of ZnO nanoparticles

UV-Vis spectroscopic measurement was carried out from 200-1100 nm and is as shown in figure 3. It shows a strong absorption band at 371nm which corresponds to a band gap of 3.43 eV. It is known that bulk ZnO has absorption at 387nm in the UV-Vis spectrum indicates that the band gap is 3.2e V. The observed blue shift may be due to size effect.

The PL spectrum of (λ_{exi}=325nm) of the ZnO at room temperature was shown in the figure. There is high emission peak at 50nm in the in the green region could be attributed to the intrinsic defects of oxygen vacancies related emission [32], as shown in the figure:4.

The ultraviolet-emission also known as near band edge emission (NBE) of the wide band gap ZnO is attributed to the exciton transition from the localized level below the conduction band to the valance band [33-34], while defect related visible emissions in ZnO nanomaterials may be ascribed to the intrinsic defects such as oxygen vacancies (Vo), Zinc vacancies (VZ_n), oxygen interstitials (O_i), Zinc interstitials (Zn_i) and oxygen antisites (OZ_n) [35-36]. A small peak is observed in the rance of 388nm, it corresponds to the violet-indigo emission is due to a radiative transition of an electron from the deep donar level of Zn_i to an acceptor level of neutral VZ_n [37] The red emission at 527nm is recognized to radiative transition of an electron from the deep donor level of Zn_i to an acceptor level caused by singly ionized charged state of the defect VZn− in ZnO [38-40]

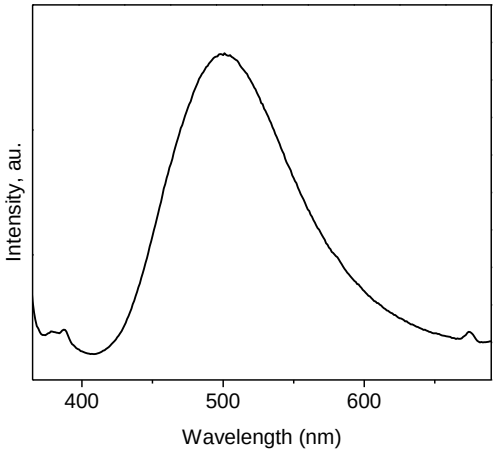

Fig. 4 Photoluminescence spectrum of ZnO nanoparticles

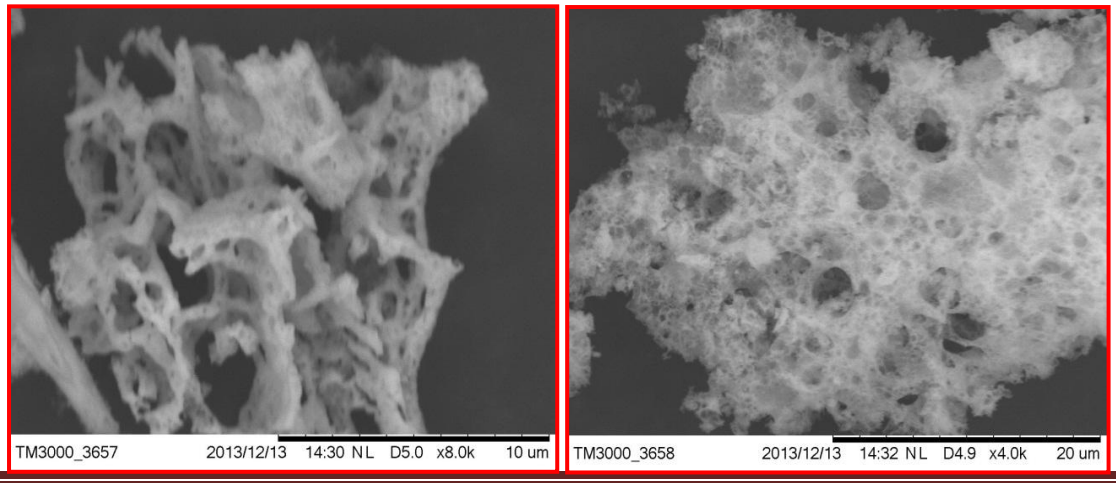

Fig. 5 SEM images of ZnO nanoparticles

The surface morphology of the prepared ZnO nanoparticles is as shown in figure 5. It can be clearly observed from low resolution, that the particles are agglomerated with irregular morphologies. The powder shows honey comb structure with broken type of hallow shells formed by the escaping gases during combustion. This type of porous network with lot of voids is typical of combustion synthesized powders due to escaping gases. These porous powders are highly friable which aids easy crushing to get hold of better particles.

Photocatalytic activity of ZnO nanoparticles

Fig.6. shows the effect of different light source on photocatalytic degradation. Two different light sources are used sun light and UV light. From the figure it is cleared that photocatalytic degradation of an azo dye is more in UV light than sun light. This is due to the fact that UV light has higher intensity (lower wavelength or higher energy), so light can easily penetrate and form more number of radicals, which increases the rate of photocatalytic degradation of an azo dye.

Antibacterial activity

The antibacterial properties of the ZnO was evaluated against Gram-ve *K. aerogenes*, *P. aeroginosa*, *P. desmolyticum*. Gram +ve bacteria *S. aureus* using agar well diffusion method. In agar well diffusion method the ZnO nanoparticles showed significant antibacterial activity on all the four bacterial strains Gram-ve *K. aerogenes*, *P. aeroginosa*, *P. desmolyticum*. Gram +ve bacteria *S. aureus* and zone of inhibition with the concentration 500 and 1000 µg per well shown in Fig.1. The data is shown in Table 1.

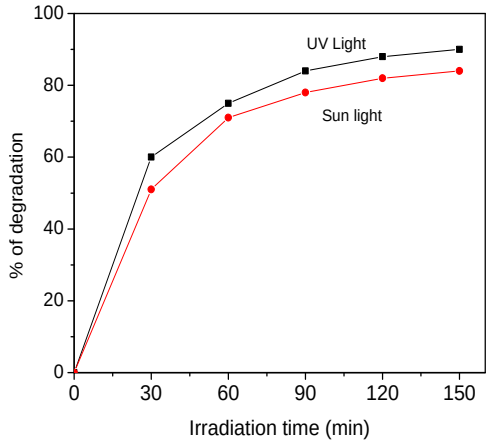

Fig. 6 Photocatalytic activity of ZnO Nps

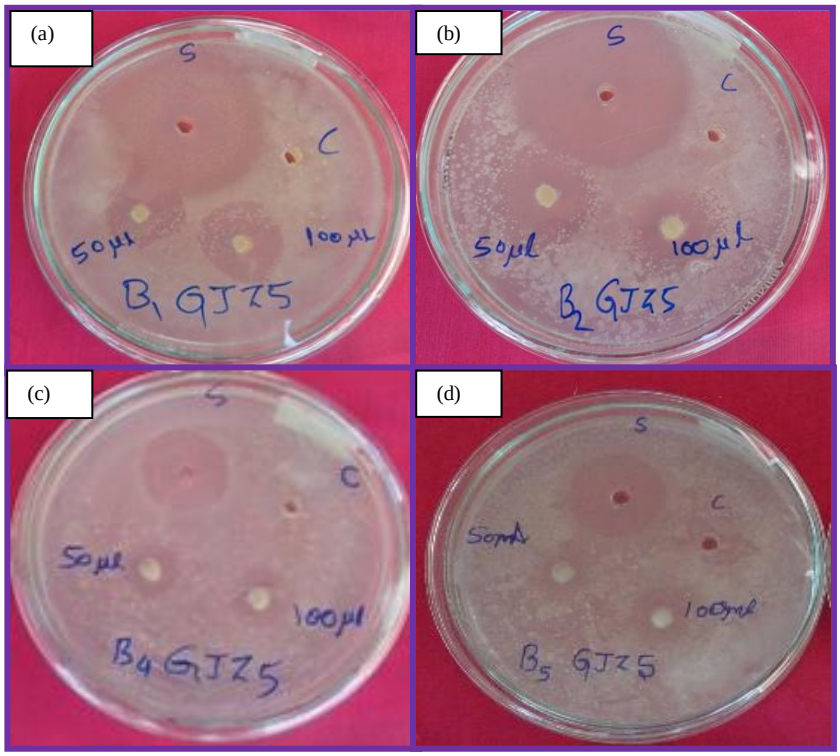

Fig. 7 (a) anti-bacterial of *Klebsiella aerogenes (b)* anti-bacterial of *Pseudomonas aeruginosa (c)* anti-bacterial of *Staphyloccus aureus* (d) anti-bacterial of *Pseudomonas desmolyticum*

Table-1: antibacterial activity of ZnO nanoparticles on pathogenic bacterial strains

Sl.no	Treatment	*Klebsiella aerogenes* (Mean±SE)	*Pseudomonas aeruginosa* (Mean±SE)	*Staphyloccus aureus* (Mean±SE)	*Pseudomonas desmolyticum* (Mean±SE)
I	Standard (5µg/50µL)	8.00±0.41	10.75±0.48	12.67±0.25	10.12±0.43
II	ZnO(PL) (500µg/50µL)	2.38±0.24**	6.75±0.32**	3.75±0.14**	2.10±0.42**
III	ZnO+(PL) (1000µg/50µL)	6.62±0.38*	9.00±0.41*	7.25±0.48**	6.12±0.31**

Values are the mean ± SE of inhibition zone. Symbols represent statistical significance,

$*P < 0.05$, $**P < 0.01$ as compared with the control group.

CONCLUSSION

We have successfully synthesized ZnO Nps via solution combustion method using novel Grape juice as a combustible fuel. XRD pattern shows that the ZnO nanoparticles are hexagonal wurtzite structure. FT-IR confirms that the presence of Zn-O at 416 cm^{-1}. UV-visible spectrum show the blue shift compared to bulk ZnO. PL spectrum reveals that strong emission peak at 502 nm. SEM Images show that the particles are agglomerated and the sizes of the nanoparticles are about 9 nm. The ZnO Nps show significant antibacterial activity against 4 bacterial strains. It also shows good photocatalytic activity for the degradation of methylene blue.

ACKNOWLEDGMENT

One of the authors Nagaraju acknowledges BMSIT for constant support and encouragement.

REFERENCES

[1]. Martin,C. R.; *Science.* 1994, *266,* 1961 [2]. Umar, A.; Hahn, Y. B.; *Am. Sci. Pub*. 2010, 5.

[3]. Aneesh, P. M.; Vanaja, K. A.; Jayaraj, M. K.; Alivov, Y. I.; Kalinina, E. V.; Cherenkov, A. E.; Look, D. C.; Ataev, B. M.; Omaev, A. K.; Chuki-Chev, M. V.; Bagnall, D. M.; *Appl. Phys. Lett.* 2003, 83, 4719.

[4]. Calestani, D.; Zha, M. Z.; Mosca, R.; Zappettini, A.; Carotta, M. C.;, Di Natale, V.; Zanotti, L.; *Sens.Actuators B-Chem.* 2010, 144, 472.

[5]. Wang, Z. L.; *Materials Science & Engineering R*—Reports 2009, 64, 33.

[6]. Xia, L. L.; Xin, T. Q.; Lu, S. C.; Chun, L. Y.; *Chin. Phys. Let.* 2005, 22, 998.

[7]. Suresh, C.; Kelly, J. M.; Ramesh, R.; Mc, D. E.; *J. Mat. Chem. C.* 2013,1, 3268.

[8]. Wang, Z. L.; *J. phys. Condense Mat*. 2004, 16, 829.

[9]. Zhong, O.P., Matijevic, E., *J. Mater. Chem.* 1996, 3, 443.

[10]. Lingna, W., Mamoun, M., *J. Mater. Chem.* 1999, 9, 2871.

[11]. Bahnemann, D.W.; Kormann, C.; Hoffmann, M.R.; *J. Phys. Chem.* 1987, 91, 3789.

[12]. Hui, Z.; Deren, Y.; Xiangyang, M.; Yujie, J.; Jin, X.; Duanlin, Q.; Nanotechnology, 2004, 15, 622.

[13]. Zhang, J.; Sun, L.D.; Yin, J. L.; Su, H. L.; Liao, C.S.; Yan, C.H.; *Chem. Mater*. 2002, 14, 4172.

[14]. Li, W.J.; Shi, E.W.; Zheng, Y.Q.; Yin, Z.W.; *J. Mater. Sci. Lett.* 2000, 20,1381.

[15]. Chen, W.; Cai, W.; Zhang, L.; Wang, G.; *J. Colloid Interface Sci.*2001, 238, 291.

[16]. Frattini, A.; Pellegri, N.; Nicastro, D.; Sanctis, O.D.; *Matter. Chem. Phys.* 2005, 94, 14.

[17]. Kuo, C.L.; Wang, C. L.; Ko, H. H.; Hwang, W. S.; Chang, K. M.; Li, W. L.; Huang, H.H.; Chang, Y. H.; Wang, M. C.; *Ceramics International.* 2010, 36, 693.

[18]. Song, R.; Liu, Y.; He, L.; *Solid State Science*, 2008, 10, 1563.

[19]. Jajarmi, P.; Materials *Letters*, 2009, 63, 2646.

[20]. Zamiri, R.; Zakaria, A.; Ahangar, H. A.; Darroudi, M.; Zak, A. K.; Drummen, G. P.; *J. of Alloys and Compounds*, 2012, 516, 41.

[21]. Deng, C.; Hu, H.; Shao, G.; Han, C.; *Materials Letters*, 2010, 64, 852.

[22]. KhorsandZak, A.; Majid, W. H. A.; Wang, H. Z.; Ramin, Y.;Moradi,A.; Golsheikh, Z. F.; *Ultrasonics Sonochemistry* 2013, 20, 395.

[23]. Yao, W.; Xiaoli Z.; Anjie , W.; Xiang, L.; Gang, W.; Lu Zhao., *Chemical Engg.Journal* ,2014, 235, 191.

[24]. Tao, Y.; Zhao, G.; Zhang, W.; Xia, S.; *Mat. Res. Bull*. 1997, 32, 501.

[25]. Nagappa, B.; Chandrappa, G. T.; *Micro and Mesoporous Mat.* 2007,106, 212. [26]. Patil, K.C.;

Chemistry of Nanocrystalline Oxide Materials. World Scientific Publishing Company, 2008.
[27]. Rasouli, S.; Sakath, S. H.; Prog. *Color Colorants Coat, 2010,3*, 19.
[28]. Sumana, K. S.; Nagabhushana, B. M;, Shivakumar, C.; Krishna Murthy, M;, Raghavendra. C.N.; *Int. J. Sci. Res*, 2012, 1, 83.
[29]. Kalyani, Y.; Kalaiselvi, N.; Muniyandi, N.; J. *Power Sources*, 2002, 111, 232.
[30]. Kalyani, P.; Int. *J. Electrochem. Sci*, 2009, 4, 30.
[31]. Perez, C.; Paul, M.; Bazerque, P.; *Acta biologiaeet Medicine Experimentalis.* 1990, 15,113.

[32]. Nagabhushana, H.; Nagabhushana, B.M.; Madesh Kumar.; Premkumar, H.B.; Shivakumara, C.; Chakradhar, R.P.S.; *Philos. Mag*, 2010, 26, 3567.
[33]. Wang, H.; Wang, H.B.; Yang, F.J.; Chen, Y.; Zhang, C.; Yang, C.P.; Li, Q.; Wong, S.P.; *Nanotechnology*, 2006, 17, 4312.
[34]. Huang, M.H.; Wu, Y.Y.; Feick, H.N.; Tran, N.; Weber, E.; Yang, P.D.; *Adv. Mater*. 2001, 13, 113.
[35]. Li, C.; Fang, G.; Fu, Q.; Su, F.; Li, G.; Wu, X.Z.; Zhao, X.,; *J. Cryst. Growth*, 2006, 19, 292.

[36]. Sun, Y.; Ndifor-Angwafor, N.G.; Riley, D.J.; Ashfold, M.N.R.; *Chem. Phys. Lett*. 2006, 431, 352.

[37]. Tatsumi, T.; Fujita, M.; Kavamoto, N.; Sasajima, M.; Horikoshi, Y.; *J. Appl. Phys*, 2004, 43, 2602.

[38]. Graces, N.Y.; Wang, L.; Bai, L.; Giles, N.C.; Halliburton, L.E.; Cantwell, G.; *Appl. Phys. Lett.* 2002, 18, 622.

[39]. Kryshtab, T.G., Khomchenko, V.S., Papusha, V.P., Mazin, M.O., Tzykunov, Y.A., *Thin Solid Films*. 2002,76, 403.

[40]. Atul Gupta.; Sunil Kumar, H.S., J.*Mater. Sci.*, *Mater. Elect*, 2010,21, 765.